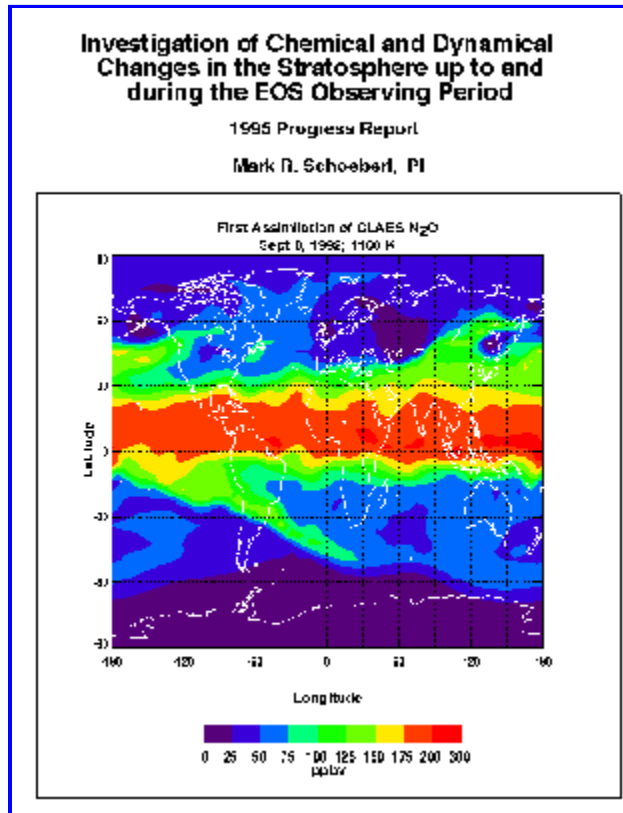


[Return to EOS page](#)

1995 Progress Report on EOS IDS



Investigation of Chemical and Dynamical Changes in the Stratosphere up to and during the EOS Observing Period

M. R. Schoeberl, P. I., *Goddard Space Flight Center*

Steve E. Cohn

Anne R. Douglass

James Gleason

Charles H. Jackman

Leslie R. Lait

Paul A. Newman

Richard B. Rood

Joan E. Rosenfield

Richard S. Stolarski

Anne M. Thompson

Goddard Space Flight Center

Marvin A. Geller

State University of New York-Stony Brook

Robert D. Hudson

University of Maryland-College Park

[Cover caption](#)

Assimilation of N₂O from Upper Atmosphere Research Satellite (UARS) Cryogenic Limb Array Etalon Spectrometer (CLAES) data. The figure shows N₂O values for 1100 K (about 5 mbar) on September 8, 1992. This is the first application of the Kalman filter assimilation technique to a trace gas scalar. See Section 2.3.2 for details.

Table of Contents

[Abstract](#)

1.0

[Background](#)

1.1

[Historical Review](#)

1.2

[Overview of Current Research Activities](#)

2.0

[Scientific Activities and Accomplishments](#)

2.1

[MODE](#)

2.2

[Stratospheric Chemical and Dynamical Modeling](#)

2.2.1

[Simulation of the Onset of Arctic Processing](#)

2.2.2

[Recovery of HCl in the Antarctic Ozone Hole](#)

2.2.3

[Trajectory Mapping](#)

- 2.2.4 [Evolution of the Pinatubo Cloud](#)
- 2.2.5 [Interactive Two-dimensional Model](#)
 - 2.2.5.1 [Global Ozone Change Due to Pinatubo](#)
 - 2.2.5.2 [Upper Stratospheric Ozone Trends](#)
- 2.3 [Stratospheric Data Assimilation](#)
 - 2.3.1 [Assimilation and Chemical Transport](#)
 - 2.3.2 [Stratospheric Constituent Assimilation](#)
- 2.4 [Tropospheric Chemistry Studies](#)
- 2.5 [Other Activities](#)
 - 2.5.1 [Radiative Transfer Work](#)
 - 2.5.2 [HIRDLS Simulation Studies](#)
 - 2.5.3 [Influence of Solar Proton Events on the Stratosphere](#)
 - 2.5.4 [TOMS data](#)
- 2.6 [Figure Captions](#)
- 2.7 [References](#)
- 3.0 [Programmatic Activities](#)
 - 3.1 [EOS Project Involvement](#)
 - 3.2 [Standard Data Products](#)
- 4.0 [Management of IDS](#)
- 5.0 [Research Directions](#)
 - 5.1 [Recent Changes](#)
 - 5.2 [Future Activities](#)
- 6.0 [Conclusions](#)
- 7.0 [List of Publications Associated with This IDS](#)
- 8.0 [EOS 1995 Budget](#)
- 9.0

Summary of Our Most Significant Recent Scientific Findings

Appendix 3.2-1

GSFC Automailer Usage Report Covering 1994-01-01 to 1994-12-31

ABSTRACT

The primary scientific goal of this EOS Interdisciplinary Science (IDS) investigation is the isolation of anthropogenic ozone changes from natural changes. To achieve these goals, we have developed an array of linked activities including model (tool) development, observational data analysis, simulation of EOS instrument measurements, and production of specialized data sets. This IDS has generated 17 years of National Meteorological Center (NMC) balanced wind data, which are being transferred to the Goddard Distributed Active Archive Center (DAAC), and maintains the trajectory automailer used worldwide. In cooperation with the Data Assimilation Office (DAO), an additional goal of this IDS and the DAO is the production of assimilated chemical data sets. As part of that effort, this IDS is responsible for the development of chemical modules and quality control of the assimilation data product.

Currently, our research focus is on the UARS data as a precursor to the EOS data sets. Among our more significant recent research results are the simulation of the historical Antarctic ozone loss using new Lagrangian chemical modeling methods and UARS observations, a new understanding of the processes behind late-winter polar chemical recovery, new results from our interactive 2-D model on the asymmetry of mid-stratosphere polar ozone trends, new insights into the transport of tropospheric pollutants, and data analysis on the impact of the Pinatubo eruption on atmospheric chemistry. This IDS investigation has also been very active within the EOS program. For example, one of our members is the EOS CHEM Project Scientist. We also have sponsored student researchers and post-doctoral investigators.

1.0 BACKGROUND

1.1 Historical Review

This EOS IDS investigation's proposed goal is to use model and observational data in the EOS and pre-EOS time frames to separate anthropogenic from natural chemical processes within the stratosphere. The original proposal included the development of a stratospheric assimilation system for meteorological and chemical data. Tropospheric chemistry was added to our proposal in the subsequent negotiation phase. With the formation of the Data Assimilation Office (DAO) at the NASA Goddard Space Flight Center (GSFC), the assimilation efforts under our proposal and the Bates/Rood proposals were combined. The current role of our IDS is to provide expertise in stratospheric data, chemical modules for the assimilation system, support in the stratospheric assimilation chemistry package, and quality control of the assimilated product. Dr. Cohn, Co-Investigator (Co-I) on the EOS assimilation proposal, was added to this investigation to strengthen the link to the DAO. We continue to have a very strong interaction with the DAO, which is collocated with most members of our group at GSFC.

1.2 Overview of Current Research Activities

[Figure 1.2-1](#) shows how we link modeling and data analysis toward the overall goals of this IDS. [Figure 1.2-2](#) shows how model development is directed, in an evolutionary sense, toward chemical

assimilation, and how our investigation draws upon other resources within the GSFC Atmospheric Chemistry and Dynamics Branch. Both figures show the distribution of Co-Is and their responsibilities among the various components of the investigation.

Fifty three publications have been sponsored or co-sponsored by this IDS. They are listed in Section 7; a non-IDS reference list for the scientific discussion in Section 2 is given in Section 2.7. The reader should consult both reference lists for Section 2.

Upper Atmosphere Research Satellite (UARS) data is the best prototype for the EOS CHEM instruments. Thus, the tools this IDS develops and our experience with UARS data are directly applicable to EOS. A large part of our team (Schoeberl, Douglass, Jackman, Rood, Geller, Newman, and Lait) is now focusing on the UARS data set as described below. Prior to the availability of UARS data, our group analyzed Total Ozone Mapping Spectrometer (TOMS) data and had a large involvement in aircraft expeditions. Members of our IDS team participated in the Airborne Arctic Stratospheric Expedition (AASE); the Second Airborne Arctic Stratospheric Expedition (AASE II); the Airborne Southern Hemisphere Ozone Experiment/Measurements for Assessing the Effects of Stratospheric Aircraft (ASHOE/MAESA); Transport and Atmospheric Chemistry near the Equator - Atlantic (TRACE-A); and the Stratospheric Photochemistry, Aerosol and Dynamics Expedition (SPADE) aircraft missions. We will also be participating in the Stratospheric Transport of Tracers (STRAT), Tropical Ozone Transport Experiment/Vortex Ozone Transport Experiment (TOTE/VOTE), and Pacific Exploratory Mission (PEM) Tropics campaigns. We believe that aircraft and satellite data are complementary and that analysis of both types of data is consistent with the interdisciplinary aspect of our proposal.

About half of our personnel resources goes to the DAO for production of their stratospheric analysis (e.g. preparation of the data and production runs of the assimilation model). Significant progress has been made on the stratospheric assimilation side as briefly reported below.

Model and data analysis tool development have been an important activity under this IDS. We have developed an interactive 2-D chemical model which we felt was needed to interpret the chemical/dynamical feedbacks in the long-term ozone trend data sets. The interactive model has significantly improved dynamics compared to the fixed dynamical model [Bacmeister *et al.*, 1995]. Preliminary results from this model will be discussed in the next section. We have also participated in the 3-D chemical modeling effort and have developed an off-line Lagrangian chemical model which is being used to simulate ozone loss in the polar regions as part of the Multiyear Ozone Depletion Experiment (MODE) under this IDS. Using the GSFC trajectory model, we also have developed a new technique to compare non-collocated trace gas data sets [Morris *et al.*, 1995; Dessler *et al.*, 1995].

In the area of tropospheric chemistry, we have focused mostly on the development of better methods for satellite retrieval of tropospheric ozone and interpretation of tropospheric ozone changes using the trajectory modeling tools developed for the stratospheric effort. Modeling of gases related to tropospheric ozone change (CH₄, CO, and NO_x) continues at a modest level.

Finally, we have performed a number of specific instrument studies for the EOS Payload Panel which included examination of the Solar Stellar Irradiance Comparison Experiment (SOLSTICE) high-resolution ultraviolet (UV) option. At Stony Brook and GSFC we are looking at the scientific impact of the High-Resolution Dynamics Limb Sounder (HIRDLS) sampling pattern on data assimilation as discussed below.

2.0 SCIENTIFIC ACTIVITIES AND ACCOMPLISHMENTS

The current ongoing research activities and some of the scientific accomplishments of this IDS are summarized in the section below. These activities indicate current extensive utilization of aircraft (e.g., ER-2, DC-8) and satellite [e.g., UARS, TOMS] data. The tools and modeling approaches we are currently developing are directed toward utilizing the upcoming EOS data sets.

Within this IDS, EOS supports a post-doc at GSFC and a graduate student at Stony Brook. During the 1995 year, we also supported the visit of Mr. Gianluca Redaelli from the Universita' degli Studi l'Aquila as a graduate student.

2.1 MODE

The goal of MODE (Multiyear Ozone Depletion Experiment) under this IDS is to simulate the observed long-term change in ozone within the polar vortex (see [Fig. 2.1-1a](#) and [2.1-1b](#)). The first phase of this experiment involves simulating the growth of the Antarctic ozone hole. This project is central to the IDS goal of isolating anthropogenic and natural changes in ozone.

To address the Antarctic problem, we are concentrating on simulating the UARS observed changes in ozone using the Lagrangian chemistry model. The procedure is as follows: first, Cryogenic Limb Array Etalon Spectrometer (CLAES) and Microwave Limb Sounder (MLS) data are mapped into potential vorticity space for data collected on August 17, 1992. Halogen Occultation Experiment (HALOE) HCl data is used from the entire previous month (because HALOE data is collected more slowly than CLAES and MLS data, we have to include the data over a longer period to get sufficient sampling with respect to potential vorticity). The UARS data are then used to initialize the Lagrangian chemical model. The model is then run forward for a month for 625 regularly spaced isentropic trajectories. The isentropic assumption is appropriate for the Antarctic vortex, as diabatic cooling rates are small [Schoeberl *et al.*, 1991; Rosenfield *et al.*, 1994, Schoeberl *et al.*, 1995]. Preliminary results are shown in [Figure 2.1-1a](#) and [2.1-1b](#). The computed ozone loss after one month's integration is comparable to that observed by MLS, and both the ClONO₂ and HNO₃ changes are similar to that observed by CLAES.

The Lagrangian chemical model currently contains no scheme for denitrification of the Antarctic vortex, but the initial CLAES values already show significant denitrification over most of the vortex region.

To examine the effect of increasing chlorine loading on the Antarctic ozone depletion, two cases are run. First, the 1992 dynamics are used for each year and only the chlorine amounts are increased. In the second case, the dynamics for each year are used along with the available chlorine.

The available inorganic chlorine is determined as a function of CH₄ using the relation of Woodbridge *et al.* [1995] and the growth rate from WMO [1995]. Because the amount of chlorine nitrate increases as the inorganic chlorine grows, the initial values of chlorine nitrate and nitric acid are linearly adjusted relative to the available inorganic chlorine (e.g., in earlier years there will be more nitric acid and less chlorine nitrate but the total NO_y (ClONO₂ + HNO₃ + NO₂ + NO + N₂O₅) observed by CLAES is assumed to be conserved).

[Figure 2.1-2](#) shows the ozone loss amounts inside the vortex as a function of year for both cases. The data are correlated with TOMS ozone amounts on September 17 for each year. The secular decline of ozone inside the vortex is clearly shown to start in the 1970s. Ozone loss is nearly linear over the 1980s, and appears to saturate in the mid-1990s. Dynamic variability appears to play little role in modifying the linear trend.

We are currently extending our methodology to the Northern Hemisphere ozone loss where we expect

similar results, but with more sensitivity to year-to-year dynamical variations.

2.2 Stratospheric Chemical and Dynamical Modeling

This section describes some of the chemical and dynamical activities supported under this IDS. The testing and development of models as tools for our science objectives and analysis of EOS data is a critical activity in the pre-EOS time frame. Most of our activity centers around analysis of satellite and aircraft data sets .

2.2.1 Simulation of the onset of Arctic processing using the 3-D chemical model

The three-dimensional chemical model is being developed under research and analysis (R&A) funding with some augmentation by the IDS. The chemical package and transport scheme eventually will be used in the chemical assimilation effort. Thus, scientific testing of the 3-D chemical model is essential for the success of the IDS assimilation program and also allows us to move toward our goal of using the 3-D chemical model for interpreting long-term trends.

The 3-D transport model, using winds and temperatures from the Goddard Data Assimilation procedure, has been used with simple representations of photochemical processes. Recently, comparisons of an ozone simulation with observations from the Total Ozone Mapping Spectrometer (TOMS) and from the MLS show that the lower stratospheric transport is realistic for a year-long integration [Douglass *et al.*, 1995a]. In an earlier study [Douglass *et al.*, 1993], the early winter activation of chlorine was simulated using a simple parameterization for HCl loss at temperatures cold enough for polar stratospheric clouds (PSCs) to form. The HCl loss was due to the heterogeneous reactions of the chlorine reservoirs HCl and ClONO₂. The difference between HCl calculated with and without this extra loss process was compared with early winter ClO observations by MLS. In no case are observed high values of ClO coincident with temperatures cold enough for PSC formation. The simulation also shows that air which has experienced cold temperatures is transported from higher latitudes to sunlit lower latitudes where high ClO is observed by MLS. The simulation shows the importance of transport to the appearance and disappearance of high values of ClO and the importance of mixing processes to the decrease in the magnitude of the ClO [Douglass *et al.*, 1993].

The critical role of transport is also shown in the work of Schoeberl *et al.* [1993a]. Analysis of the UARS MLS observations in early January 1992 shows a clear relationship between predicted polar stratospheric cloud (PSC) formation along back trajectories and elevated ClO amounts. These findings are in good agreement with previous analysis of aircraft observations [Schoeberl *et al.*, 1993b]. The observed decrease in ClO following a PSC encounter agrees with the decrease calculated using a photochemical model, provided the calculation accounts for the movement of the parcel. Schoeberl *et al.* [1993a] also showed that the occasional high values of ClO seen by MLS outside the polar vortex are accounted for by statistical fluctuations in the MLS data retrieval.

There have been substantial improvements to the 3-D chemistry and transport model in the last year. Development of a complete scheme for stratospheric photochemical processes, including gas-phase and heterogeneous reactions and a model for PSC formation, allows a more complete comparison of modeled physical processes with observations. Fig. 2.2.1-1 shows HNO₃ and aerosol extinction as observed by CLAES, and HNO₃ and aerosol surface area as modeled by the CTM. High values of HNO₃ are apparent within the model vortex in both the observations and in the simulation; the model values are somewhat lower than observed. There is a low area of HNO₃ in the model and in the observations, indicating the sequestering of nitric acid in the form of aerosols. This is supported by the maximum in aerosol extinction as seen by CLAES, and the maximum in the model NAT surface area.

[Figure 2.2.1-2](#) shows very low values of both chlorine reservoirs HCl and ClONO₂ within the polar vortex, indicating nearly complete conversion of chlorine reservoirs to ClO, the dimer Cl₂O₂, and Cl₂. Comparison of simulations such as this one with observations provide important information concerning the mechanisms of lower stratospheric ozone loss.

2.2.2 Recovery of HCl in the Antarctic ozone hole

One advantage of the UARS data set is that many of the key stratospheric constituents are observed by at least one of the instruments. It is possible to combine observations from different instruments by accounting for dynamical variability. This technique was first used by Schoeberl *et al.* [1989] as potential vorticity (PV) mapping. PV mapping is one of the types of tools we can apply to EOS data sets. The mapping technique and its power in interpreting chemical observations is demonstrated by an analysis of CLAES observations of ClONO₂ and HNO₃; HALOE observations of ozone, HCl, NO, and NO₂; and MLS observations of ozone and ClO [Douglass *et al.*, 1995b].

Maps of ClO, ClONO₂, HNO₃, and ozone for the Northern and Southern Hemispheres show the major differences which lead to the formation of the ozone hole. In the Southern Hemisphere, deep within the polar vortex, the HNO₃ is removed from the stratosphere. ClO levels are high, ClONO₂ values are low, and ozone depletion is drastic. Nearer to the vortex edge, temperatures generally are still cold enough to produce nitric acid trihydrate (NAT) PSCs, but not cold enough for ice clouds. Both HNO₃ values and ClONO₂ values are large in this region, forming a "collar" surrounding the inner vortex. ClO, while elevated, is much lower than deep within the vortex.

In the Northern Hemisphere, low values of HNO₃ are found only when NAT PSCs are actually present. High values of ClONO₂ and moderate O₃ loss are seen at the end of the winter. It was originally thought that the photochemistry of the Northern Hemisphere would resemble the photochemistry of the collar region.

Time series of ozone, ClO, ClONO₂, HNO₃, NO, NO₂, HCl, and temperature are produced by averaging the observations at constant potential temperature (constant entropy and modified potential vorticity). The results are shown in [Figures 2.2.2-1](#) and [2.2.2-2](#) for the Northern and Southern Hemisphere. In the Northern Hemisphere, ClO is low, ClONO₂ and HNO₃ are high. There is little evidence for loss of ozone. The NO seen by HALOE is significantly lower than the NO₂; HCl shows an expected slow rise as the chlorine reservoirs seek their normal balance. Throughout most of the spring, ClONO₂ is the principal chlorine reservoir.

In the Southern Hemisphere collar, ClO is elevated throughout the UARS southern yaw period, producing steady loss of ozone. However, the ClONO₂ does not rise, in spite of the sunlight and the high values of HNO₃. Instead, when the ozone falls below about 0.5 ppmv, the HCl starts to rise rapidly. Also during this time period, NO rises rapidly. These observations allow identification of the responsible chemical mechanism. When ozone falls to low values, the reaction to produce ClO (Cl + O₃) and to produce NO₂ (NO + O₃) both become less important. The concentration of Cl rises because the loss of Cl is reduced (Cl + O₃). Furthermore, the production of Cl is increased (NO + ClO) because of a decrease in the loss rate of NO (NO + O₃). Thus, production of HCl through Cl + CH₄ rises non-linearly. HCl becomes the dominant reservoir for chlorine in the Southern Hemisphere spring due to low ozone.

2.2.3 Trajectory mapping

The trajectory mapping technique developed under this IDS [Morris *et al.*, 1995] is another powerful

new procedure developed under this IDS which can be used to effectively collocate data measured at different times and places. Trajectory mapping has applications to data assimilation and will make an important contribution to validation of the EOS data sets. We have already applied the technique to UARS data sets.

To begin trajectory mapping, we initialize a parcel at each measurement time and then move the parcel forward (or backward) in time using a trajectory model. The method makes maximum use of the data over a short period of time and compares favorably with Kalman, Salby-Fourier methods, and PV reconstruction techniques [Schoeberl and Lait, 1992]. The additional advantage of trajectory mapping is that missing data can be handled easily and the maps can be made at any synoptic time. Both measurement and associated errors can be advected for later combination or comparison with new measurements. Using trajectory mapping, we have been examining the systematic differences in instrument measurements. As an example, [Figure 2.2.3-1](#) shows comparisons between MLS and HALOE water vapor data at different potential temperature surfaces from Morris *et al.* [1995]. These measurements are non-coincidental and are brought together using trajectory mapping. The trajectory mapping technique reveals a bias between the measurements.

Since the trajectory mapping technique also allows us to bring together non-coincident measurements (such as those made by UARS HALOE, MLS, and CLAES), we have been able to use this information to show the consistency of the observed chlorine budget with the modeled chlorine budget in the lower stratosphere [Dessler *et al.*, 1995].

One of the problems with trajectory mapping [Morris *et al.*, 1995] and trajectory domain filling methods [Fisher and O'Neill, 1993] has been the inability to produce a regular grid at synoptic times. A variant of the domain filling technique developed by our group and Sutton *et al.* [1994] generates a regular grid from the trajectories. We refer to this method as Reverse Domain Filling (RDF) [Schoeberl and Newman, 1995; Newman and Schoeberl, 1995]. Instead of filling the domain with parcels and running the model forward in time, a regular grid of parcels are laid down at the final time and run backwards. The data taken at the earlier time are then interpolated onto the irregular distribution of parcels. [Figure 2.2.3-2](#) shows results using the RDF technique. High-resolution PV maps generated using RDF and the standard NMC analysis are shown for the same day. To generate this RDF map, data from 10 days earlier are trajectory mapped. The dramatic improvement in the apparent resolution of the trace gas fields can be used to test the sampling strategy of HIRDLS as discussed in Section 2.5.2 below.

2.2.4 Evolution of the Pinatubo cloud

The measurements of EOS AM's Measurements of Pollution in the Troposphere (MOPITT) instrument will produce low vertical resolution CO profiles and column CH₄ measurements. The Ozone Dynamic Ultraviolet Spectrometer (ODUS), scheduled for the EOS CHEM payload, will produce column ozone. We have developed a new method using trajectories which allows us to reconstruct the vertical structure of trace gases from column measurements under certain conditions. The column can be thought of as a shadow or projection of the three-dimensional field. The time evolution of the projection along with the column information can be used to reconstruct the three-dimensional field. We combine the various projections (like a medical CAT scan) to estimate the three-dimensional structure. The technique is an improvement of the method originally developed by Schoeberl *et al.* [1992c].

The new technique has been applied to the SO₂ field from the Pinatubo cloud as measured by TOMS. First, a column of trajectory parcels are initialized over the domain of the cloud at a large number of potential temperature surfaces forming a cylinder. The parcels are advected forward in time. The projection of the parcels is compared with SO₂ measured by TOMS during this period. The initial cloud is then systematically edited by comparing the collocation of the trajectory "shadows" with the

observations. [Figure 2.2.4-1](#) shows the Pinatubo cloud 3 days post-eruption after editing 15 days of data. Backtracking the edited cloud, we get good agreement with the eruption times.

This calculation serves two purposes. First, we see the development and dispersal of the eruption cloud in three dimensions. Second, the method utilizes assimilation winds in the tropics. Tests with NMC balance winds show we are unable to generate an eruption cloud consistent with TOMS data using balanced wind fields derived from NMC data. Thus, this method is sensitive to the wind fields, and provides a test of the assimilation winds in the tropics.

2.2.5 Interactive two-dimensional model

Under this IDS, we have developed an interactive 2-D model based on the dynamics package of Bacmeister and Schoeberl [Bacmeister *et al.*, 1995] to study long-term trends in trace gases. This model fully couples chemistry dynamics and radiation, and thus can be used to study the feedbacks between the processes which we have not been able to study with the fixed circulation 2-D model. Over the last year, the model's troposphere has been extensively tuned and the radiation routines upgraded. The chemistry package will be upgraded within the coming year to become compatible with the chemical packages used by the 2-D assessment model.

2.2.5.1 Global ozone change due to Pinatubo

The 2-D Interactive Model has most recently been used in a preliminary study of the effects of the Mt. Pinatubo aerosol cloud on stratospheric ozone and temperatures. The radiative perturbation gave rise to a tropical temperature rise of almost 2 K, as well as an altered circulation with more upwelling in the low latitudes and downwelling in the middle and high latitudes. [Figure 2.2.5.1-1](#) shows the latitudinal distribution of the column ozone changes resulting from the inclusion of the volcanic aerosol in both the radiation and the chemistry. The computed low latitude column ozone depletions of 1-2% result from a combination of the upwelling due to the radiative perturbation with the losses due to heterogeneous chemistry. In the high latitudes, depletions as large as 6% in the Northern Hemisphere and 50% in the Southern Hemisphere are predicted, due mainly to heterogeneous chemistry occurring on the aerosol surfaces. The large Southern Hemisphere high latitude perturbation is likely due to the fact that the model contains no PSCs. If PSCs were present in both the background and the volcanic aerosol runs, chlorine would already have been activated in the background and the volcanic impact would not likely be so large.

[Figure 2.2.5.1-2](#) shows the daily differences of the globally averaged column ozone amounts from the background case. The modeled differences of 2-3% up until the autumn of 1992 are in reasonable agreement with observations [Gleason *et al.*, 1993]. However, the model ozone starts recovering earlier than observations. In the next development phase, we plan to incorporate in the model heterogeneous reactions on the surface of PSCs, and include solar cycle effects, which need to be taken into account in order to be able to compare model results with observations.

2.2.5.2 Upper stratospheric ozone trends

The 2-D Interactive Model also is being used currently to understand the hemispheric differences between upper stratospheric ozone trends. Ozone trends calculated using SBUV/SBUV2 satellite observations exhibit a pronounced asymmetry between the Northern and Southern Hemispheres in the 1 mbar region. This can be seen in [Figure 2.2.5.2-1a](#), which plots the annual average ozone trend in %/year calculated from 11.6 years of zonally averaged SBUV measurements. The Southern Hemisphere trend is larger in magnitude than the Northern Hemisphere trend, peaking above 1.3 %/year. In contrast, the Northern Hemisphere peak is about 1.0 %/year. In addition to being about 30% larger than the

Northern Hemisphere trend, the Southern Hemisphere peak also occurs at about 1 mbar compared to the Northern Hemisphere peak at about 2 mbar. The large gradient in the trend between the equator and polar regions has been attributed to the large methane gradient at that altitude [Hood *et al.*, 1993], but the asymmetry has not yet been explained. It is believed to be real, and not simply an artifact of the retrieval algorithm [McPeters, private communication].

Modeling studies of the upper stratospheric ozone trend show that they result from increases in stratospheric chlorine loading. However, the GSFC 2-D Fixed Transport Model which had been used in such calculations, does not exhibit any asymmetry. [Figure 2.2.5.2-1b](#) shows the trend in ozone calculated by the GSFC 2-D Fixed Transport Model when the background chlorine in the model is increased from 2.0 to 3.3 ppbv. In contrast to current 2-D models, the GSFC 2-D Interactive Model does exhibit an asymmetric trend, as shown in [Figure 2.2.5.2-1c](#). Although the altitude and the magnitude of the calculated trend does not agree well with the SBUV observations, determination of the reason for the model asymmetry may indicate the source of the asymmetry seen in the SBUV-calculated trends.

In the GSFC 2-D Interactive Model, the Southern Hemisphere increase in ClO in the trend calculation is significantly larger than the Northern Hemisphere increase. Since the rate of chlorine-catalyzed ozone loss is proportional to ClO, larger Southern Hemisphere increases in ClO will result in larger Southern Hemisphere trends. In the model, the Southern Hemisphere ClO increase is larger than the Northern Hemisphere increase even though the total odd chlorine increase is similar in both hemispheres. The Interactive Model thus indicates that the partitioning of the Cly family is different in the two hemispheres.

At 1 mbar, almost all of Cly is either in the form of ClO or HCl. The partitioning of the family at this altitude will therefore be determined by the ClO/HCl ratio, which is inversely proportional to CH₄. Therefore, if CH₄ is low, Cly will be predominantly in the form of ClO. If CH₄ is high, Cly will be in the form of HCl. It follows that if there is an asymmetry between the Northern and Southern Hemispheres in CH₄, with lower values of CH₄ in the Southern Hemisphere, the Southern Hemisphere Cly partitioning will favor ClO and the Southern Hemisphere trend will be larger than the Northern Hemisphere trend. The Interactive Model does show this asymmetry between Northern and Southern Hemisphere CH₄ concentrations, and this is the primary cause of the trend asymmetry in the model.

The mechanism responsible for the asymmetric trend in the Interactive Model may also be operating in the real atmosphere. Preliminary results indicate that there is an asymmetry in CH₄ between the Northern and Southern Hemispheres, suggesting that the trend asymmetry seen in the SBUV data is due to an asymmetry in CH₄ concentrations. [Figure 2.2.5.2-1d](#) shows zonally-averaged CH₄ observations from the CLAES instrument. The Northern Hemisphere data is an average of observations taken between September 21, 1992 and January 9, 1993. The Southern Hemisphere data is averaged over the March 23, 1992 to July 13, 1992 time period. The seasonal behavior of the SBUV trends shows that the trend is maximized during these periods in the Northern and Southern Hemispheres, so it is during these time periods that the CH₄ asymmetry would be important. The CH₄ concentrations in the Southern Hemisphere at 1 mbar are clearly about 30% lower than the Northern Hemisphere values.

Because CH₄ is a long-lived tracer, its distribution in a model of the stratosphere will be primarily determined by the model dynamics. The source of the asymmetry in trace gas distributions is due the weaker planetary wave forcing which is characteristic of the Southern Hemisphere and which results in less eddy mixing in the upper stratospheric polar region. The consequence is an asymmetric CH₄ distribution which produces asymmetric trends. This work is currently being prepared for publication.

2.3 Stratospheric Data Assimilation

The stratospheric assimilation effort is focused on two activities, traditional meteorological assimilation, and constituent assimilation. Both of these are core activities of the Data Assimilation Office (DAO). The meteorological analyses (and forecasts) are used for both trajectory and chemical transport models, as well as flight planning in the aircraft missions. The constituent efforts are in their early stages, but have already contributed to advancement of Kalman filter data assimilation methods.

Accomplishments in the stratospheric assimilation effort include:

1. A three-and-one-half-year UARS assimilation
2. Operational support of the SPADE, ASHOE/MAESA, and STRAT campaigns
3. Use of the assimilation in successful multi-year 3-D transport chemistry applications
4. Assimilation of UARS temperature observations
5. New assimilation methodologies to improve stratospheric wind estimates
6. A theoretical study of the impact of the HIRDLS scanning
7. Kalman filter constituent assimilation
8. The use of assimilation winds in chemical assessments.

2.3.1 Assimilation and chemical transport

The highlights have been the production of a three and a half year data set starting at the time of the launch of the Upper Atmosphere Research Satellite (UARS) and operational support of the ASHOE/MAESA aircraft campaign. The UARS period assimilation has been used in the three-dimensional stratospheric chemistry model discussed above. A notable accomplishment is a one-year integration of ozone using parameterized chemistry. [Figure 2.3.1-1](#) shows the annual cycle of total ozone from the ozone integration, TOMS data, and a typical 2-D model [see Douglass *et al.*, 1995a]. The ability of the assimilation model to simulate the annual cycle is a notable achievement, and increases the credibility of assessment applications of models.

A second application in the 3-D chemistry effort has shown that the assimilation winds represent dynamical variability with sufficient accuracy to allow direct quantitative comparison with the UARS data. In addition, the fact that the model/UARS correlations are maintained on seasonal time scales increases the confidence that the chemistry transport model provides an accurate representation of the atmosphere during the period that the UARS instrument is not observing poleward of 34° latitude in each hemisphere. A recent application is the study of Kawa *et al.* [1995] focusing on missing nitrogen chemistry in the upper stratosphere.

The operational support of the ASHOE/MAESA and STRAT missions provided forecasts for flight planning and assimilation analyses to aid in the interpretation of the constituent observations. For flight planning, the forecasts are used with contour advection and RDF trajectory calculations to predict high resolution features in the constituent fields. The Goddard Earth Observing System (GEOS) forecasts were comparable to United Kingdom Meteorological Office (UKMO) and European Center for Medium Range Weather Forecast (ECMWF) products and superior to NMC.

The applications of the GEOS fields to chemistry and transport problems provide stringent tests of the assimilation and direct attention to shortcomings that need improvement. Two problems which appear common to all stratospheric meteorological analyses are: a warm bias at polar latitudes during extremely cold periods, and poor representation of instantaneous winds in the subtropics. In addition, the studies have revealed two persistent, possibly related, polar problems in the GEOS system that are probably artifacts of the data assimilation system. These two polar problems are excessive noise at the pole, especially when there is cross-polar flow, and a persistent upward signal in the residual circulation at the

South Pole. The polar problems could be related to the assimilation system or some conceptual error in the formulations of the system. If an artifact of the assimilation system, then the problem could be related to the assimilation model or the analysis routine.

Recently the noise problems have been eliminated by using grid rotation to eliminate the polar singularity. There have been significant improvements in the representation of the residual circulation, though more research is needed to achieve the same level of quality that has been obtained with the previous system. The residual circulation is more difficult to calculate accurately. Present approaches involve all aspects of the assimilation system, with a emphasis on removing artifacts of the data insertion process.

The warm bias at cold polar temperatures is very likely related to data problems, combined with a natural tendency for the model to underestimate the most extreme events. To address this bias, temperature data from UARS MLS has been assimilated. While this shows some improvement, data boundaries due to the UARS scanning pattern are proving problematic with conventional assimilation techniques (but see next section).

In addition to proper location of dynamical systems and seasonal transitions, the data assimilation does contain a quasi-biennial oscillation (QBO). The QBO remains elusive in general circulation model (GCM) simulations. Because of the superior characteristics of the transport calculations, winds from the GEOS assimilation are being used in 3-D assessments of the impact of stratospheric aircraft. This represents an important contribution of the EOS effort to the quest to assess environmental change.

2.3.2 Stratospheric constituent assimilation

Constituent assimilation has a special role in the assimilation effort. It not only should provide a scientifically useful data product, but constituent assimilation provides an effective mechanism to build advanced assimilation capabilities. The role of constituent assimilation, plans, and interactions with NMC are described in the Data Assimilation Office Plan (available from R. Rood). Initial experiments with an idealized model have focused on the impact of the scanning capabilities of HIRDLS, compared with the single profile limb view of the UARS instruments. First results show that the scanning capability of HIRDLS does allow effective filling in of the tracer spectra (also see Section 2.5.2).

In early 1995, the world's first assimilation of UARS N₂O on isentropic surfaces was completed. This is the first Kalman filter data assimilation of a global geophysical field. Because of the computational demands, the assimilation was run on the 512 node Intel/Paragon at JPL. The effort has been reported in Lyster *et al.* [1995].

[The figure on the cover of this report](#) shows the N₂O field for September 8, 1992 at 1100 K. This is the period when UARS is looking southward. Note the tongue of high N₂O being drawn from the subtropics into middle and high southern latitudes and the continuous tongue of low N₂O air being drawn from middle latitudes [see Randel *et al.*, 1993]. The spatial continuity of these fields is more realistic than from the mapped product alone. Especially exciting is the plot north of 34°. There are no CLAES observations in this region. Initial verification of the structure in the Northern Hemisphere has been accomplished using Improved Stratospheric and Mesospheric Sounder (ISAMS) data, which can provide pole-to-pole coverage. The major features verify well. This also reveals the potential to use the structure information from ISAMS in future assimilations.

2.4 Tropospheric Chemistry Studies

The tropospheric chemistry effort is now utilizing the tools developed for stratospheric chemical and dynamical analysis including the trajectory models and the assimilated data. With the launch of EOS AM, MOPITT CO and CH₄ data will be analyzed using the tools and techniques developed to analyze TRACE-A data discussed below. Two current activities in the tropospheric chemistry area are (1) use of models to evaluate the role of convection in stratospheric-tropospheric exchange and ozone formation; and (2) development of tropospheric ozone satellite products. Both of these efforts are also supported by the NASA R&A program.

In the area of convection, the multi-scale study of midwest convection (comparison of GEOS-1 and GCE-scaled up mass fluxes; GCE = Goddard Cumulus Ensemble model) was published [Pickering *et al.*, 1995a] and a similar analysis completed for a tropical mesoscale convective event during TRACE-A [Wang *et al.*, 1995]. Implementation and evaluation of the RAS (Relaxed Arakawa-Schubert) parameterization in the GEOS-1 transport scheme are in progress [Allen *et al.*, 1995]. Variations in tropospheric Radon-222 data, signifying convective impact on transport at a number of tropical and mid-latitude sites, are well-simulated for a one-year simulation in 1991-92 and for shorter periods covered during intensive experiments (e. g. during 1987 STEP-Tropical experiment).

An important accomplishment during this year has been a unique application of models, *in situ* and satellite (TOMS and AVHRR) data to quantify causes of the observed south tropical Atlantic tropospheric ozone maximum in the GTE/TRACE-A aircraft mission period (September-October 1992). Major EOS-relevant results of these studies are summarized in the following paragraphs.

A significant milestone in proving convective-chemistry linkage was achieved with the clear identification of upper tropospheric cloud outflow of biomass burning pollutants (NO_x, CO, hydrocarbons) in the TRACE-A data set [Pickering *et al.*, 1995b]. Both GCE and MM5 simulations reproduce upper tropospheric carbon monoxide (CO) levels observed in TRACE-A Flight 6 (27 Sept. 1992, staged from Brasilia). The MM5 simulation shows how widespread is the effect of convective redistribution ([Figure 2.4-1a](#) and [2.4-1b](#)). The impact of convective outflow for ozone formation over the South Atlantic Basin is considerable. By comparing two ozone soundings downwind of TRACE-A Flight 6 (at Natal on the Atlantic coast, 28 and 30 Sept. 1992), an increase in middle and upper tropospheric ozone (of 20-30 ppbv in some layers) could be traced to parcels originating in convective biomass-burning regions ([Figure 2.4-2a](#) and [2.4.2b](#)). The CO-NO_x-HC composition of the cloud outflow air masses easily supports 5-6 ppbv/day ozone formation or ~3-4 Dobson units in the 8- to 12-km layer after four days, roughly the time it takes to reach the Atlantic.

Besides experimental confirmation of post-convection elevated ozone formation (previously only inferred from pre-convection observations and models), the TRACE-A Flight 6 analysis suggests a strong role for lightning in the tropical upper tropospheric NO_x budget. We estimate that 30-40% of the NO_x in cloud-processed air masses of that flight was due to lightning [Pickering *et al.*, 1995b].

A more general estimate of the impact of deep convection on South Atlantic ozone is derived from analysis of the sources of high ozone layers in 72 soundings taken at Natal, Ascension Island, and three southern Africa sites during the TRACE-A. Defining "excess" ozone to be the amount above average non-burning-season ozone, it was found that 20-30% of excess ozone in the South Atlantic Basin in September-October 1992 originated from South American regions active in biomass burning and convection [Thompson *et al.*, 1995a]; the remainder (at low-mid tropospheric levels) was from southern Africa.

In the category of remote sensing, derivation of tropical tropospheric ozone from TOMS [Hudson *et al.*, 1995] led to regional analysis for the TRACE-A period [Kim *et al.*, 1995a; Thompson *et al.* 1995b; 1996]. We estimate that the minimum averaging time for these maps is 7-10 days. A comparison of 1-15

October 1989 and 1-15 October 1992 for the tropical band (10° N - 14° S) shows that in the northern equatorial Atlantic 1992 was 5-15 DU higher than for 1989 [Kim *et al.*, 1995b]. For southern Africa, AVHRR data [Justice *et al.*, 1995] show that the 0-10° S band had 2-3 times more fires in early October 1992 than for 1989. However, low level flows from these fires head south of the high ozone difference area [Sieber *et al.*, 1995].

Current projects with the TOMS-derived tropospheric ozone product include (1) processing of all 1992 data (twice-monthly maps) to study seasonal variability and the evolution of that year's ozone maximum; sondes for validation are available year-round at Natal, Ascension, Brazzaville and Irene (Pretoria, SA); and (2) processing the entire TOMS data set (1979-1992) to study interannual variability and to deduce any trends in the tropical band. There is no evidence of a total ozone trend in the tropics [Stolarski *et al.*, 1991], but without this product we cannot exclude the possibility that during the 1980's stratospheric ozone decreased while tropospheric ozone increased.

Improvement of tropospheric ozone estimates is an ongoing project with this IDS. We are also working with MLS ozone from UARS and TOMS data to estimate the tropospheric ozone residual.

2.5 Other Activities

The section below summarizes some of the other activities supported by this IDS. These research efforts do not fall under the categories described above but are an important part of this investigation.

2.5.1 Radiative transfer work

Heating rates computed with a radiation model and NMC temperature observations were used in a one-dimensional vortex interior descent model to determine diabatic descent rates for the fall and winter periods in the Northern Hemisphere for 1988-89 and 1991-94, and in the Southern Hemisphere for 1987 and 1992 [Rosenfield *et al.*, 1995]. The computed descent rates generally agree well with observations of long-lived tracers [Rosenfield *et al.*, 1994; Strahan *et al.*, 1994], thus validating the radiative model. These results argue against the "flowing processor" concept of the polar vortex, which would require much larger cooling rates than those computed.

Several molecules important in the chemistry of the stratosphere photodissociate in the Schumann-Runge bands of oxygen, a spectral region in which the penetration of solar radiation into the middle atmosphere varies by several orders of magnitude as a function of wavelength. It has been suggested that a knowledge of the fine structure of the solar spectrum is therefore necessary for an accurate calculation of photolysis rates for these molecules. The SURE option proposed for the EOS SOLSTICE instrument was designed to provide measurements of the solar UV fine structure. Computations of the sensitivity of the computed photolysis rates to the solar spectral resolution show that knowledge of the fine structure in the Schumann-Runge region of the solar spectrum produces only a marginal (1 -2 %) difference in the computation of photolysis rates [Rosenfield, 1995]. As a result of these computations, we recommended that the EOS Payload Panel drop the high resolution UV spectrometer option for SOLSTICE.

An ongoing project is to study the radiative and dynamical effects of the Pinatubo volcanic aerosol. A parameterization of the optical thicknesses of both the background and the volcanic aerosol has been developed for use in our wide band radiative transfer model. Stratospheric Aerosol and Gas Experiment II (SAGE II) observations of one-micron extinctions, along with Mie calculations of absorption and extinction cross sections using observed particle size distributions for the sulfate aerosol, have been used. The volcanic aerosol perturbation was included in our 2-D interactive model by imposing monthly, latitudinally varying fields of aerosol extinction coefficients and surface area densities. The 2-

D model studies of this volcanic perturbation are described in Section 2.2.5.1. Currently the aerosol fields which are imposed on the model are tied to 1 micron SAGE II extinctions and a single measured particle size distribution. We plan to improve the spatial and temporal distributions of the aerosols, and their absorption and extinction spectrum, by combining the SAGE II aerosol data set with other data sets, including Stratospheric Aerosol Measurement II (SAM II) and UARS.

2.5.2 HIRDLS simulation studies

The HIRDLS instrument on the EOS CHEM platform is designed to make horizontal and vertical observations at higher resolutions than have previously been made, while observing the upper troposphere and lower stratosphere with improved sensitivity and accuracy. The higher horizontal resolution is achieved by azimuthal scanning of the instrument's field of view. Previous limb-viewing sounders (LIMS, ISAMS, CLAES, MLS, etc.) did not have this azimuthal scanning capability and thus were unable to sample a given latitude circle more than twice per orbit.

In this study, we attempt to determine what degree of improvement HIRDLS' horizontal scanning capability yields in creating gridded maps of constituent fields. This is done by sampling model output using the anticipated HIRDLS sampling pattern, gridding the simulated satellite measurements thereby obtained, and comparing the resulting gridded fields to the originals.

One simulation, performed at SUNY, used as its original fields the output temperature of the Goddard STRATAN effort and ozone from the 3-D Chemical-Transport Model (CTM); these fields had a relatively low resolution (4° latitude by 5° longitude), so they were interpolated to a 2- by 2.5-degree grid before being sampled on the 85 and 10 mb pressure surfaces by a scanning and non-scanning modeled HIRDLS instrument. The 2- by 2.5-degree model fields were also put onto a 1- by 1-degree grid using a simple isentropic transport model; scanning and non-scanning HIRDLS sampling then were done on the 465 and 850 K potential temperature surfaces. Next, these simulated satellite soundings were used to reconstruct gridded horizontal maps via bilinear interpolation. The results for a single day (January 22, 1992) indicate, as expected, that the maps obtained from scanning HIRDLS samples exhibit more detail than in those derived from the non-scanning samples. In addition to visual inspection of the maps, root mean square (RMS) differences were calculated between the model ozone fields and the scanning HIRDLS' maps ("RMS-S"), and between the model ozone fields and the non-scanning HIRDLS' maps ("RMS-NS"); the former are about 20% lower than the latter. When calculated for temperature fields, on the other hand, RMS-NS values were about 30% lower than RMS-S, indicating that maps made from non-scanning HIRDLS samples are somewhat superior for temperature; the reason appears to be that the temperature field's broader-scale structures were oversampled by the scanning HIRDLS near the pole as they evolved with time. A more sophisticated gridding technique such as Kalman filtering, which takes into account the asynoptic nature of the data, might reduce this effect.

A second simulation used high resolution trace gas fields instead of the lower resolution model data; several days varying by season were examined instead of one day, and a measure of the statistical reliability of the results also has been performed. The high-resolution fields were simulated using the Reverse Domain Filling technique (described in section 2.2.3) to put nitrous oxide (N₂O) measurements from the UARS CLAES instrument on a 1 by 1 degree grid for subsequent HIRDLS sampling. Three potential temperature surfaces were used: 465 K, 560 K, and 850 K, covering the lower to middle stratosphere. One day for each season in each hemisphere was selected for analysis and comparison.

Visual comparisons of plots of the original data with the two mapped fields show, for some of the days, striking improvements of the scanning HIRDLS over a non-scanning HIRDLS ([Fig. 2.5.2-1](#)). Filaments in the original fields are clearly visible in the gridded maps from the scanning instrument; the larger-scale structure, too, appears to be more accurately depicted. For other days, however, the improvement

seems less pronounced. Visual inspection, though, while useful, can provide little more than anecdotal evidence for any improvements due to azimuthal scanning. Application of a standard sign test shows that the differences are indeed statistically significant to within the 99% confidence level.

A quantitative comparison using RMS differences is desirable, but these are of limited use without a measure of their uncertainty. Therefore, an estimate of their uncertainties was obtained by calculating RMS values from randomly selected subsets of the available data grid points. The spread in those calculations can be used as a measure of their uncertainty. Table 1 shows the RMS differences and their uncertainties for both the scanning and non-scanning HIRDLS for each day. As in the STRATAN/CTM simulation, the RMS-S differences are typically between 20 to 30 percent lower than the corresponding RMS-NS differences.

Table 1 also shows how the RMS differences change with latitude. As the orbits come closer together near the poles, one would expect the differences between scanning and non-scanning HIRDLS maps to become smaller there. In general, this is true, but there are exceptions apparently related to strong gradients or filamentary structures very near the pole.

Future plans involve creating a full month of high-resolution N₂O fields taken every six hours. These will be sampled by the simulated HIRDLS instrument as time varies, instead of taking the instantaneous snapshot of the current study. These asynoptic soundings will be subjected to the Salby space-time Fourier transform procedure to create synoptic maps without aliasing small or fast-moving features. While HIRDLS' azimuthal scanning will not improve the resolution of such maps, it should make them more robust, as one can average the six more or less independent spectra from the six scan positions to achieve a 60% reduction in noise.

TABLE 1: RMS differences for Northern Hemisphere

465 K SURFACE	00-90 :	00-30 :	30-60 :	60-90 :
1992-02-28				
S	17.6 +/- 3.6	12.7 +/- 1.9	16.9 +/- 3.1	22.3 +/- 3.9
NS	22.6 +/- 3.9	15.7 +/- 2.0	23.7 +/- 3.9	29.0 +/- 3.9
Spring				
1992-05-15				
S	17.6 +/- 4.7	11.9 +/- 2.7	20.5 +/- 4.5	19.8 +/- 5.3
NS	25.3 +/- 6.0	16.2 +/- 2.6	30.8 +/- 5.8	28.2 +/- 5.3
Summer				
1992-07-27				
S	9.8 +/- 3.5	11.2 +/- 2.9	12.1 +/- 3.8	2.3 +/- 0.5
NS	14.5 +/- 3.6	16.4 +/- 4.1	17.3 +/- 3.7	3.2 +/- 0.6
Fall				
1992-10-21				
S	18.6 +/- 4.5	18.6 +/- 5.0	24.8 +/- 4.1	7.5 +/- 5.9
NS	25.5 +/- 5.7	24.0 +/- 5.4	33.1 +/- 4.6	12.0 +/- 6.2

2.5.3 Influence of solar proton events on the stratosphere

Our work on solar proton events (SPEs) is also related to the overall goals of this IDS. SPEs can cause natural changes in the atmosphere on relatively short time-scales (days to months). We have investigated the effects of the extremely intense SPEs of October 1989 with both our 2-D and 3-D model. In Jackman *et al.* [1993, 1995] we noted the importance of properly representing the polar vortices and warming events and the importance of the interannual variations in the downward transport when studying the atmospheric effects of the SPEs weeks to months after the events. We also showed that our simulations of the polar NO_x increases during the SPEs are close to observations (both rocket and SAGE II) and that these large SPEs can have a significant impact on polar lower stratospheric NO_x a few months after the events. Such large natural perturbations to the polar stratosphere are the anthropogenically-caused polar changes observed in the Antarctic spring.

2.5.4 TOMS data

Aside from UARS data, investigators under this IDS spend some time looking at TOMS data and performing analysis of global ozone amounts. Simulations of ozone change have to fit within the TOMS observational set. We are currently continuing our analysis of the ozone hole data. [Figure 2.5.4-1](#) shows the size of the ozone hole averaged between mid-September and mid-October. The size is basically the area enclosed within the 220 DU contour. Preliminary 1994 data show that the size is comparable to that in the previous three years. The ozone hole size appears to have stabilized to a fraction of the vortex area as predicted by Schoeberl and Hartmann [1991]. Our analysis of the TOMS data is also beginning to focus on the results of the MODE experiment discussed in section 2.1. A TOMS-like instrument (ODUS) will be launched on EOS CHEM.

Critics of the anthropogenic chlorine theory for south polar ozone loss frequently point to the ozone hole of 1958 as proof that the ozone hole is natural. Newman [1994] has shown that the Dumont d'Urville data showing the existence of the 1958 ozone hole was inconsistent with data from near by bases and is not self-consistent. That work, supported by this IDS, closes another argument by regulatory critics.

2.6 Figure Captions

Figure 2.1-1. Maps comparing the Lagrangian chemical model results for 1992 with observations. (a) The change in ozone observed by MLS (lower maps) is compared with the Lagrangian model computed ozone changes (upper maps). (b) Model computed changes in ClONO₂ and HNO₃ are compared with CLAES observed changes in ClONO₂ and HNO₃. Also shown are model MPV (modified potential vorticity) fields and HCl fields.

Figure 2.1-2. Average ozone change inside the vortex from August 17 to September 17 computed with the Lagrangian chemical model as a function of year. The dynamics is held as 1992 dynamics and only the stratospheric chlorine amounts changed for the cases shown as triangles. The crosses are cases that include the dynamics for the indicated year. Also shown are the average August 17 total ozone values from TOMS for the region interior of the 220 DU contour (filled circles).

Figure 2.2.1-1. CLAES HNO₃ and aerosols (plots on left) compared to 3-D chemical model computations (plots on right) for January 9, 1992 at 45 mb (hPa).

Figure 2.2.1-2. Three-dimensional chemical model simulation of chlorine species for January 11, 1992 at 45 mb (hPa). Upper maps show the active chlorine species, ClO, Cl₂O₂, and Cl. The lower maps show the reservoirs, HCl and ClONO₂.

Figure 2.2.2-1. Southern Hemisphere time series for observations from MLS (ozone, ClO), CLAES

(HNO₃, ClONO₂) and HALOE (ozone, HCl, NO, NO₂) binned by MPV. The bottom panel contains the time series of the average and minimum latitude of the observations, as well as for the average temperatures (taken from NMC) for the points within the MPV (modified potential vorticity) band indicated.

Figure 2.2.2-2. Same as 2.2.2-1 but for the Northern Hemisphere.

Figure 2.2.3-1. Comparison of water vapor measurements from UARS HALOE and MLS using the trajectory mapping method. Symbols represent the different potential temperatures [Morris *et al.*, 1995].

Figure 2.2.3-2. Comparison of trajectory RDF and standard NMC-analyzed PV fields for January 12, 1992 at 1100 K. Note the dramatic increase in detail.

Figure 2.2.4-1. Three-dimensional reconstruction of the Mt. Pinatubo eruption cloud after three days using trajectory editing of the TOMS SO₂ data.

Figure 2.2.5.1-1. The latitudinal distribution of the column ozone changes resulting from the inclusion of the volcanic aerosol in both the radiation and the chemistry. This result is from the interactive 2-D model.

Figure 2.2.5.1-2. The daily differences of the globally averaged column ozone amounts from the background case (in percent) after the eruption of Pinatubo. Interactive 2-D model is solid line; TOMS observations are dashed.

Figure 2.2.5.2-1. (a) The annual average ozone trend in %/year calculated from over 11 years of zonally averaged SBUV measurements. (b) The trend in ozone calculated by the GSFC 2-D fixed transport model when the background chlorine in the model is increased from 2.0 to 3.3 ppbv. (c) The interactive 2-D (coupled) model trend. (d) Zonally-averaged CH₄ observations from the CLAES instrument.

Figure 2.3.1-1. The daily difference between the zonal mean total ozone at 46°N taken from TOMS, the 3-D Chemical transport model (Exp 654) which uses the assimilation winds, and from the Goddard standard 2-D Model (Dobson Units).

Figure 2.4-1. MM5 simulation results for CO tracer. (a) Mixing ratios at 1200 UT September 27, 1992 at 11 km. Region shown is fine-grid domain of MM5 simulation (30-km resolution). Includes grid-scale and subgrid transport. (b) Frequency distributions of CO measurements from DC-8 (three-minute averages, equivalent to approximately 40 km travel distance) and MM5-simulated values at 11 km in the region 6.5-10 S, 44-49 W.

Figure 2.4-2. (a) Ozonesonde profiles taken at Natal, Brazil on September 28 and 30, 1992. Note large increase in ozone mixing ratios between 11 km and tropopause. (b) Forward trajectories using ECMWF data from points on Flight 6 flight track in cloud outflow at 11.3 km and 9.5 km. Trajectories (solid lines) shown with positions noted every 12 hours. Lighter dashed lines are trajectories initialized in 2.5 degree by 2.5 degree cluster surrounding central point.

Figure 2.5.2-1. Improvement in trace gas observations expected with HIRDLS horizontal scanning. Upper figure is a height-resolution RDF simulation of N₂O using UARS CLAES data. Using HIRDLS in a non-horizontal scanning mode, and sampling the field shown in the upper figure, the field at the lower right is obtained. Using the scanning capability, the field at the lower left is obtained.

Figure 2.5.4-1. Size of the ozone hole computed from TOMS vs. year (solid line) with error bars compared to the size of the vortex at 450 K (dashed line). Error bar in 1986 indicates the uncertainty in the size of the vortex which is approximately the same for each year.

2.7 References

These are references which are not included in the list of IDS publications given in Section 7.

Fisher, M., and A. O'Neill, Rapid descent of mesospheric air into the stratospheric polar vortex, *Geophys. Res. Lett.*, 20, 1267-1270, 1993.

Gleason, J. F., P. K. Bhartia, J. R. Herman, R. McPeters, P. A. Newman, R. S. Stolarski, L. Flynn, G. Labow, D. Larko, C. Seftor, C. Wellemeyer, W. D. Komhyr, A. J. Miller, and W. Planet, Record low global ozone in 1992, *Science*, 260, 523-526, 1993.

Hood, L. L., R. D. McPeters, J. P. McCormack, L. E. Flynn, S. M. Hollandsworth, and J. F. Gleason, Altitude dependence of stratospheric ozone trends based on Nimbus 7 SBUV data, *Geophys. Res. Lett.*, 20, 2667-2670, 1993.

Justice C. O., J. D. Kendall, P. R. Dowty, and R. J. Scholes, Satellite remote sensing of fires during the SAFARI campaign using NOAA-AVHRR data, *J. Geophys. Res.*, in press, 1995.

Randel, *et al.*, Stratospheric transport from the tropics to middle latitudes by planetary wave mixing, *Nature*, 365, 533-537, 1993.

Schoeberl, M. R., *et al.*, Reconstruction of the constituent distribution and trends in the Antarctic polar vortex from ER-2 flight observations, *J. Geophys. Res.*, 94, 16815-16845, 1989.

Schoeberl, M. R., and L. R. Lait, Conservative coordinate transformations for atmospheric measurements, in *Tools in Atmospheric Science, Proceedings of the International School of Physics "Enrico Fermi"*, G. Visconti and J. Gille, Editors, Italian Physical Society, 1992.

Stolarski, R. S., P. Bloomfield, R. D. McPeters, and J. R. Herman, Total ozone trends deduced from Nimbus 7 TOMS data, *Geophys. Res. Lett.*, 19, 159-162, 1991.

Sutton, R. T., H. Maclean, R. Swinbank, A. O'Neill, F. W. Taylor, High resolution stratospheric tracer fields estimated from satellite observations using Lagrangian trajectory calculations, *J. Atmos. Sci.*, 51, 2995-3005, 1994.

Weaver, C. J., A. R. Douglass, and R. B. Rood, Thermodynamic balance of three-dimensional stratospheric winds derived from a data assimilation procedure, *J. Atmos. Sci.*, 50, 2987-2993, 1993.

WMO, *Scientific Assessment of Ozone Depletion: 1994, Report No. 37*, World Meteorological Organization Global Ozone Research and Monitoring Project, 1995.

Woodbridge, E. L. *et al.*, Estimates of total organic and inorganic chlorine in the lower stratosphere from in situ and flask measurements during AASE II, *J. Geophys. Res.*, 100, 3057-3064, 1995.

3.0 PROGRAMMATIC ACTIVITIES

3.1 EOS Project Involvement

This IDS has performed a number of programmatic duties associated with the EOS effort. Dr. Schoeberl was the first Atmospheres Panel chairman (1990-1993) and became the first EOS CHEM Project Scientist for most of FY 1994. Dr. Gleason, was added to the IDS team in 1994 and became the EOS CHEM Project Scientist in August 1994.

This IDS has been heavily involved in the EOS restructuring/rebaselining/reshaping programs. For example, we have conducted and are performing specific instrument studies for the Payload Panel (see Sections 2.5.1, 2). Drs. Newman and Lait have served on EOSDIS committees. In July 1994, Dr. McNeal, the HQ Program Scientist, and our IDS sponsored a workshop to familiarize the science community with measurements on EOS CHEM. The workshop report has been published in the Earth Observer. This IDS is now involved in the 1995 EOS reshape activity, the PI is the lead author of Chapter 9 of the Science Implementation Plan.

3.2 Standard Data Products

This IDS presently produces two data products. First, we generate and transfer to the DAAC the NMC balance wind data set which includes heights, balanced winds, temperatures, and potential vorticity. Transfer of the data set from 1979-August 1995 will start in September, 1995; currently we have nearly finished debugging the transfer and conversion software. Second, this IDS supports the GSFC Automailer trajectory model. The automailer is a scheme by which NASA and non NASA users can generate forward and back trajectories for analysis of aircraft and satellite data. The automailer also supports visualization of meteorological data files - support for that activity is under the R&A program. To use the automailer, the requester e-mails a request to a special account. This starts a job on one of the EOS supported workstations which computes the trajectory using NMC balanced winds. The results are then e-mailed back to the requester. This facility will soon be available on our home page. Appendix 3.2-1 shows the national and international usage of the GSFC Automailer.

Early in this IDS investigation we developed a self documenting data formatting scheme called DF [Lait *et al.*, 1993]. This scheme is similar to HDF (although HDF was developed at the time, there were few tools for HDF). The DF scheme has been very popular and we have used it to provide general access to satellite, aircraft and ground-based data sets within the IDS. Our experience with DF has given us valuable insights into self-documenting storage schemes.

4.0 MANAGEMENT OF IDS

Most of the co-investigators are located at GSFC and are collocated. The exceptions are Dr. Hudson at the University of Maryland, Dr. Geller at the University of New York at Stony Brook, and Dr. Cohn who is located at the DAO off-site facility. The team has formal meetings roughly quarterly, but communicates informally every day as needed.

Within the IDS, the PI assumes the responsibility for overall research activities. As indicated in Figure 1.1-1 and 1.1-2, individual team members work on various aspects of the project. Dr. Rood is in charge of the data assimilation component, while Dr. Douglass works on the 3-D chemical model, the Lagrangian chemical model, and UARS data analysis. Dr. Jackman is in charge of the 2-D modeling work and Dr. Rosenfield heads the group effort on the interactive 2-D model. Dr. Lait, who is currently working on the HIRDLS sampling pattern with Dr. Geller, is also responsible for maintenance of the IDS home page and the trajectory automailer. Dr. Lait also supports aircraft mission data analysis and NMC analysis. Dr. Stolarski, Dr. Newman, and Dr. Gleason work on the analysis of TOMS data. Dr.

Newman also analyses aircraft and UARS data and is in charge of moving the NMC balanced wind data to the Goddard DAAC. Dr. Thompson works on tropospheric chemistry. Dr. Hudson is developing tropospheric ozone retrieval algorithms.

5.0 RESEARCH DIRECTIONS

5.1 Recent Changes

With the availability of UARS data, the IDS has shifted much of its focus from aircraft data and NMC analysis to UARS and assimilation data analysis. Both of these changes have been made because of the wider availability and improved quality of both UARS and assimilation data sets. Research directions have also changed with the increase in workstation computer power, cheap mass storage in the form of 10 gigabyte disk drives, and the availability of the new Interactive 2-D model and Lagrangian chemical model tools. This shift has allowed us to plan and undertake investigations (such as MODE, section 2.1) that were previously only possible with the more computationally costly 3-D model.

5.2 Future Activities

In general, our research focus is shifting away from polar processes toward understanding the mechanism producing the mid-latitude ozone trends. We have also begun to focus on the lower stratosphere, especially the processes associated with strat-trop exchange, tropical mid-latitude interaction, and upper tropospheric physical processes. This change in focus draws closer together the troposphere and the stratosphere chemical efforts, and is phased to take advantage of the availability of MOPPIT observations on EOS AM as well as data from the STRAT ER-2 missions. Over the next two years we will be completing the MODE effort and improving the interactive 2-D model's troposphere and mesosphere. We intend to apply the trajectory mapping technique to a wider range of UARS data such as investigating the NO_y budget in a manner similar to the Cly analysis of Dessler *et al.* [1995], and the searching for filamentary structures in the high horizontal resolution ATLAS - CHRISTA limb sounding data. Our investigation of EOS instrument performance will also continue.

A number of the tools we have developed for the stratosphere are currently being tested in the troposphere. Recently we have applied the RDF technique to tropospheric water vapor observed by GOES. We find that the fine scale structure in the upper tropospheric water vapor seen by GOES can be well simulated using assimilation analysis (or forecasts) augmented by 3 day RDF calculations. This effort is actually part of a broader research effort we have begun with the Hartmann IDS and Dr. James Anderson at Harvard University, to understand the role of water vapor in the tropical upper tropopause using the Perseus remotely piloted aircraft (RPA).

6.0 CONCLUSIONS

Since this IDS task was begun (in 1990) there has been considerable progress. The scientific direction remains the same: the isolation of man-made from natural chemical changes in the atmosphere and the understanding of their mechanisms. But, we have broadened our scope to include tropospheric chemical processes, and we are branching out to begin studying water vapor in the upper troposphere using our stratospheric transport tools. Our overall focus has been on tool and model development for interpretation of EOS and non-EOS data. We also have a very close collaboration with the EOS data assimilation effort. Our most active current research focus is on the analysis of available satellite and aircraft data sets (UARS, TOMS, STRAT, SPADE, etc.). Two new models have been recently developed under this IDS, the Lagrangian chemical model and the coupled 2-D model. We support

development efforts in radiative transfer, the 3-D chemical model, and the trajectory model. Our present data products include balanced wind, potential vorticity and height fields from NMC data, and trajectories to order from the GSFC trajectory automailer.

Our IDS effort has been very active within the EOS program. One of our members is the EOS CHEM Project Scientist, the PI has headed the Atmospheres Panel, has been involved in several of the EOS rescope activities, and is in charge of a Science Implementation Plan Chapter. Our Co-Is head the EOS data assimilation panel and serve on EOSDIS advisory committees. We also have an active program in instrument evaluation with an eye to efficient observing strategy or instrument problems. Our IDS currently supports a post-doc at GSFC and a student at Stony Brook.

Our near term future research activities involve continued analysis of available satellite and aircraft data, a larger focus on stratosphere-troposphere interaction, and a tropospheric chemical modeling.

7.0 LIST OF PUBLICATIONS ASSOCIATED WITH THIS IDS

(all 53 of these references were sponsored or co-sponsored by this IDS)

Allen, D., R. B. Rood, A. M. Thompson, and R. D. Hudson, Three-dimensional Rn-22 calculations using assimilated data and a convective mixing algorithm, submitted to *J. Geophys. Res.*, 1995.

Bacmeister, J. T., M. R. Schoeberl, M. E. Summers, J. E. Rosenfield, and X. Zhu, Descent of long-lived trace gases in the winter polar vortex, *J. Geophys. Res.*, *100*, 11669-11684, 1995.

Chappellaz, J. A., I. Y. Fung, and A. M. Thompson, Atmospheric methane increase since the last glacial maximum, 1. Source, Estimates, *Tellus*, *45B*, 228-241, 1993.

Dessler, A. E. *et al.*, Correlated observations of HCl and ClONO₂ from UARS and implications for stratospheric chlorine partitioning, *Geophys. Res. Lett.*, *22*, 1721-1724, 1995.

Douglass, A., R. Rood, J. Waters, L. Froidevaux, W. Read, L. Elson, M. Geller, Y. Chi, M. Cerniglia and S. Steenrod, A 3-D simulation of the early winter distribution of reactive chlorine in the north polar vortex, *Geophys. Res. Lett.*, *20*, 1271-1274, 1993.

Douglass, A. R., C. J. Weaver, R. B. Rood, and L. Coy, A three-dimensional simulation of the ozone annual cycle using winds from a data assimilation system, *J. Geophys. Res.*, in press, 1995a.

Douglass, A. R., M. R. Schoeberl, R. S. Stolarski, J. W. Waters, J. M. Russell III, and A. E. Roche, Inter-hemispheric differences in springtime deactivation of vortex ClO, *J. Geophys. Res.*, *100*, 133967-13978, 1995b.

Hudson, R. D., J. Kim, and A. M. Thompson, On the derivation of tropospheric column ozone from radiances measured by the Total Ozone Mapping Spectrometer, *J. Geophys. Res.*, *100*, 11137-11145, 1995.

Jackman, C. H., J. E. Nielsen, D. J. Allen, M. C. Cerniglia, R. D. McPeters, A. R. Douglass, and R. B. Rood, The effects of the October 1989 solar proton events on the stratosphere as computed using a three-dimensional model, *Geophys. Res. Lett.*, *20*, 459-462, 1993.

Jackman, C. H., M. C. Cerniglia, J. E. Nielsen, D. J. Allen, J. M. Zawodny, R. D. McPeters, A. R. Douglass, J. E. Rosenfield, and R. B. Rood, Two-dimensional and three-dimensional model simulations, measurements, and interpretation of the influence of the October 1989 solar proton events on the middle atmosphere, *J. Geophys. Res.*, *100*, 11641-11660, 1995.

Jacob, D. J., *et al.*, The origin of ozone and NO_x in the tropical troposphere: A photochemical analysis of aircraft observations over the South Atlantic Basin, submitted to *J. Geophys. Res.*, 1995.

Kawa, S. R., D. W. Fahey, J. C. Wilson, M. R. Schoeberl, A. R. Douglass, R. S. Stolarski, E. L. Woodbridge, H. Jonsson, L. R. Lait, P. A. Newman, M. H. Proffitt, D. W. Toohey, D. E. Anderson, M. Loewenstein, K. R. Chan, C. R. Webster, R. D. May, and K. K. Kelly, Interpretation of NO_x/NO_y Observations from AASE-II using a model of chemistry along trajectories, *Geophys. Res. Lett.*, *20*, 2507-2510, 1993.

Kawa, S. R., J. Kumer, A. Douglass, A. Roche, S. Smith, F. Taylor, and D. Allen, Missing chemistry of reactive nitrogen in the upper stratospheric polar vortex, *Geophys. Res. Lett.*, in press, 1995.

Kim, J. H., R. D. Hudson, and A. M. Thompson, Derivation of time-averaged tropospheric column ozone from radiances measured by the Total Ozone Mapping Spectrometer: Intercomparison and analysis, submitted to *J. Geophys. Res.*, 1995a.

Kim, J. H., R. D. Hudson, and A. M. Thompson, A new method of deriving tropospheric column ozone from TOMS radiances: October 1989 and 1992, in *Biomass Burning and Global Change* (Chapman Conference Book), J. S. Levine, Editor, submitted, 1995b.

Lait, L. R., E. R. Nash and P. A. Newman, DF: A proposed data format standard, NASA Tech. Memo., 4467, 1993.

Lait, L. R. , An alternative form of potential vorticity, *J. Atmos. Sci.*, *51*, 1754-1759, 1994.

Lehmann, P. , D. J. Karoly, P. A. Newman, T. S. Clarkson, and W. A. Matthews, Long-term winter total ozone changes at Macquarie Island, *Geophys. Res. Lett.*, *19*, 1459-1462, 1992.

Lyster, P. M., S. E. Cohn, R. Menard, L.-P. Chang, S.-J. Lin, and R. Olsen, An implementation of a two-dimensional filter for atmospheric chemical constituent assimilation on massively parallel computers, submitted to *Mon. Wea. Rev.*, 1995.

Morris, G. *et al.*, Trajectory mapping and applications to data from the upper atmosphere research satellite, *J. Geophys. Res.*, in press, 1995.

Nash, E. R., P. A. Newman, J. E. Rosenfield, and M. R. Schoeberl, An objective determination of the polar vortex using Ertel's potential vorticity, submitted to *J. Geophys. Res.*, 1994.

Newman, P. A., and M. R. Schoeberl, A reinterpretation of the data from the NASA Stratosphere-Troposphere Exchange Project, *Geophys. Res. Lett.*, in press, 1995.

Newman, P. A., Antarctic total ozone in 1958, *Science*, *264*, 543-546, 1994.

Nielsen, J. E., R. B. Rood, A. R. Douglass, M. C. Cerniglia, D. A. Allen, Loewenstein, M., J. Podolske, D. Fahey, E. Woodbridge, P. Tin, A. Weaver, P. Newman, S. Strahan, S. Kawa, M. Schoeberl, and L.

- Lait, New observations of the NO_y/N₂O correlation in the lower stratosphere, *Geophys. Res. Lett.*, *20*, 2531-2534, 1993.
- Pickering, K. E., A. M. Thompson, D. P. McNamara, and M. R. Schoeberl, An intercomparison of isentropic trajectories over the South Atlantic, *Monthly Wea. Rev.*, *122*, 864-897, 1994.
- Pickering, K. E., A. M. Thompson, W-K. Tao, R. B. Rood, D. P. McNamara, and A. M. Molod, Vertical Transport by convective clouds: Comparisons between cloud-scale and global-scale models, *Geophys. Res. Lett.*, *22*, 1089-1092, 1995a.
- Pickering, K. E., A. M. Thompson, Y. Wang, W-K. Tao, D. P. McNamara, V. W. J. H. Kirchhoff, B. G. Heikes, G. W. Sachse, J. D. Bradshaw, G. L. Gregory, and D. R. Blake, Convective transport of biomass burning emissions over Brazil during TRACE-A, submitted to *J. Geophys. Res.*, 1995b.
- Plumb, R. A., D. W. Waugh, R. J. Atkinson, P. A. Newman, L. R. Lait, M. R. Schoeberl, E. V. Browell, A. J. Simmons, M. Loewenstein, and D. W. Toohey, Intrusions into the lower stratospheric Arctic vortex during the winter of 1991/92, *J. Geophys. Res.*, 1993.
- Redaelli, G., L. Lait, M. Schoeberl, P. A. Newman, G. Visconti, A. d'Alturio, F. Masci, V. Rizi, L. Froidevaux, J. W. Waters, A. J. Miller, UARS MLS O₃ soundings compared with lidar measurements using the conservative coordinates reconstruction technique, *Geophys. Res. Lett.*, *21*, 1535-1538, 1994.
- Rosenfield, J. E., The radiative feedback of polar stratospheric clouds on Antarctic temperatures, *Geophys. Res. Lett.*, *20*, 1195-1198, 1993.
- Rosenfield, J. E., P. A. Newman, and M. R. Schoeberl, Computations of diabatic descent in the stratospheric polar vortex, *J. Geophys. Res.*, *99*, 16677-16689, 1994.
- Rosenfield, J. E., The sensitivity of stratospheric photodissociation rates to the solar spectral resolution in the Schumann-Runge Bands, *J. Atm. Terr. Phys.*, *57*, 843-855, 1995.
- Schoeberl, M. R., and D. L. Hartmann, The dynamics of the stratospheric polar vortex and its relation to the springtime ozone depletions, *Science*, *251*, 46-52, 1991.
- Schoeberl, M. R., R. S. Stolarski, A. R. Douglass, P. A. Newman, L. R. Lait, J. W. Waters, L. Froidevaux, and W. G. Read, MLS ClO observations and Arctic polar vortex temperatures, *Geophys. Res. Lett.*, *20*, 2861-2864, 1993a.
- Schoeberl, M. R., A. R. Douglass, R. S. Stolarski, P. A. Newman, L. R. Lait, D. Toohey, L. Avallone, J. G. Anderson, W. Brune, D. W. Fahey, and K. Kelly, The evolution of ClO and NO along air parcel trajectories, *Geophys. Res. Lett.*, *20*, 2511-2514, 1993b.
- Schoeberl, M. R., S. D. Doiron, L. R. Lait, P. A. Newman, A. J. Krueger, A simulation of the Cerro Hudson SO₂ cloud, *J. Geophys. Res.*, *98*, 2949-2955, 1993c.
- Schoeberl, M. R., M. Luo, J. M. Russell III, and J. E. Rosenfield, An analysis of the Antarctic HALOE trace gas observations, *J. Geophys. Res.*, *100*, 5159-5172, 1995.
- Schoeberl, M. R., and L. C. Sparling, Trajectory modeling, diagnostic tools in *Atmospheric Physics, Proceedings of the International School of Physics "Enrico Fermi"*, G. Fiocco and G. Visconti, Editors,

Italian Physical Society, 289-304, 1995.

Schoeberl, M. R., and P. A. Newman, A multiple level trajectory analysis of vortex filaments, *J. Geophys. Res.*, in press, 1995.

Sieber, C., J. H. Kim, R. D. Hudson, and A. M. Thompson, Time-averaged tropospheric ozone derived from TOMS radiances: A comparison of maps for the tropical Atlantic from 1-15 Oct. 1989 and 1-15 Oct. 1992, *Eos*, Trans. AGU, 25 Apr. 1995 Suppl., S72, 1995.

Smyth, S., *et al.*, Factors influencing the upper free tropospheric distribution of reactive nitrogen over the south Atlantic during the TRACE-A experiment, submitted to *J. Geophys. Res.*, 1995.

Strahan, S. E., J. E. Rosenfield, M. Loewenstein, J. R. Podolske, and A. Weaver, The evolution of the 1991-2 Arctic vortex and comparison with the GFDL 'SKYHI' general circulation model, *J. Geophys. Res.*, 99, 713-723, 1994.

Talbot, R., *et al.*, Chemical characteristics of continental outflow over the tropical south Atlantic Ocean from Brazil and southern Africa, submitted to *J. Geophys. Res.*, 1995.

Thompson, A. M., J. A. Chappellaz, I. Y. Fung, and T. L. Kucsera, Atmospheric methane increase since the last glacial maximum, 2. Interactions with oxidants, *Tellus*, 45B, 242-257, 1993a.

Thompson, A. M., K. E. Pickering, D. P. McNamara, and R. D. McPeters, Effect of marine stratocumulus on TOMS ozone, *J. Geophys. Res.*, 98, 23051-23057, 1993b.

Thompson, A. M., Aspects of modeling the tropospheric hydroxyl radical concentration, *Israel J. Chem., Special Issue on Atmospheric Chemistry*, 34, 277-287, 1994a.

Thompson, A. M., Measuring and modeling the tropospheric hydroxyl radical (OH), *J. Atmos. Sci., Special AMS OH Symposium Issue*, in press, 1994b.

Thompson, A. M., Photochemical Modeling of Chemical Cycles: Issues related to the interpretation of ice core data, in *Biogeochemical Cycles and Ice Cores*, R. Delmas, Editor, Springer-Verlag, in press, 1995.

Thompson, A. M., K. E. Pickering, D. P. McNamara, M. R. Schoeberl, R. D. Hudson, J. H. Kim, E. V. Browell, J. Fishman, V. W. J. H. Kirchhoff, and D. Nganga, Where did tropospheric ozone over southern Africa and the tropical Atlantic come from in October 1992? Insights from TOMS, GTE/TRACE-A and SAFARI-92, submitted to *J. Geophys. Res.*, 1995a.

Thompson, A. M., R. D. Diab, G. E. Bodeker, M. Zunckel, G. Coetzee, C. Archer, K. E. Pickering, D. P. McNamara, J. Combrink, J. Fishman, and D. Nganga, Total ozone over Southern Africa and the adjacent Atlantic during SAFARI-92, *J. Geophys. Res.*, SAFARI Special Issue, in press, 1995b.

Thompson, A. M., T. Zenker, G. E. Bodeker, and D. P. McNamara, Ozone over southern Africa: Patterns and influences, in *Fire in Southern African Savanna: Ecological and Atmospheric Perspectives*, J. A. Lindsay, M. O. Andreae, P. D. Tyson, and B. van Wilgen, Editors, Univ. of Witwatersrand Press, in press, 1996.

Waugh, W. D., R. A. Plumb, R. J. Atkinson, M. R. Schoeberl, L. R. Lait, P. A. Newman, M

Loewenstein, D. W. Toohy, and C. R. Webster, Transport of material out of the stratospheric Arctic vortex by Rossby Wave Breaking, *J. Geophys. Res.*, 1993.

Wang, Y., W-K. Tao, K. E. Pickering, A. M. Thompson, R. Adler, J. Simpson, P. Keehn, G. Lai, Mesoscale (MM5) simulations of TRACE-A and PRE-STORM convective events, submitted to *J. Geophys. Res.*, 1995.

8.0 EOS 1995 BUDGET

Budget information has been deleted from this copy.

9.0 SUMMARY OF OUR MOST SIGNIFICANT RECENT SCIENTIFIC FINDINGS

The list below summarizes our most recent and significant recent scientific findings.

(1) We believe that we have discovered the explanation for the observed asymmetry in ozone trends in the upper stratosphere. The differences are apparently due to the different dynamics in the two hemispheres. The larger, broader descent over the Antarctic winter pole leads to lower methane amounts compared to the Arctic. This is a finding from the new Interactive 2-D model which was developed under this IDS (Section 2.2.5.2, Fig. 2.2.5.2-1). This work is currently being prepared for publication.

(2) Our second major discovery is of the anomalous growth in HCl inside the Antarctic vortex after the ozone depletion [Douglass *et al.*, 1995]. This discovery came from our work with the UARS data, and the use of PV analysis tools and the Lagrangian chemical model that were developed by this IDS. Our analysis showed that once ozone disappears in the Antarctic polar vortex, the balance between Cl and ClO shifts toward Cl. Cl then attacks methane forming HCl. The HCl rise is observed in the UARS HALOE data. This result was later confirmed by the ASHOE/MAESA aircraft expedition (Section 2.2.2, Figs. 2.2.2-1,2).

(3) Our third significant result is the first quantitative simulation of the historical Antarctic ozone hole. This study uses the new Lagrangian chemical model combined with UARS data. Our simulation shows that the Antarctic ozone depletion development matches observations from UARS. Using chlorine estimates from previous years, we have been able to show that the secular decline in Antarctic ozone is consistent with TOMS observations and that dynamics plays little role in the secular trend (Section 2.1, Figs. 2.1-1,2). This work is currently being prepared for publication.

Appendix 3.2-1

GSFC /science Automailer Usage Report
Covering 1994-01-01 to 1994-12-31

USER ACCESSES

cadyp@aer.com	16	johnson@grizzly.uwyo.edu
wyojim@sovusa.com	3	zhao@wolf.uwyo.edu
zhang@asrcss2.asrc.albany.edu	152	deshler@mcmsun5.mcmurdo.gov
atmosphys@uwyo.edu	5	voemelho@mcmsun5.mcmurdo.gov
awhitten@uwyo.edu	13	hamill@light.arc.nasa.gov
lj@mercul.gps.caltech.edu	32	taba@sky.arc.nasa.gov
cbrock@cassandra.cair.du.edu	48	westphal@halo.arc.nasa.gov
manderbe@cassandra.cair.du.edu	25	huahu@laserspec1.cc.espo.nasa.gov
psulliva@diana.cair.du.edu	12	lait@triffid.cc.espo.nasa.gov
xliu@diana.cair.du.edu	6	root@notus.cc.espo.nasa.gov
dan@bottesini.harvard.edu	5	theory@fermi.cc.espo.nasa.gov
elliott@bottesini.harvard.edu	32	gregg@skye.gsfc.nasa.gov
eric@bottesini.harvard.edu	17	huahu@vs4000.jpl.nasa.gov
ewg@triton.harvard.edu	48	jjm@mark4sun.jpl.nasa.gov
ham@triton.harvard.edu	2	chip@mirage.larc.nasa.gov
hintsa@huarp2.harvard.edu	1	hervig@teton.larc.nasa.gov
kab@triton.harvard.edu	10	mcinerny@hops.larc.nasa.gov
theory@triton.harvard.edu	1	bjohnson@cmdl.noaa.gov
psulliva@du.edu	7	johnson@cmdl1.cmdl.noaa.gov
dcheng@uars.sunysb.edu	824	voemel@cmdl.noaa.gov
dshindell@uars.sunysb.edu	28	s107a.mcmurdo@mcmurdo.gov
lemmons@uars.sunysb.edu	20	s148b.mcmurdo@mcmurdo.gov
screwell@uars.sunysb.edu	42	adriani@hp.ifs.fra.cnr.it
vyudin@uars.sunysb.edu	1	didonfra@hp.ifs.fra.cnr.it
xpeng@uars.sunysb.edu	72	fromm@poam_a.nrl.navy.mil
ychi@uars.sunysb.edu	128	hornstei@poamb.nrl.navy.mil
jamesw@acd.ucar.edu	47	mas@atlas.nrl.navy.mil
katja@ash.mmm.ucar.edu	150	poam@poam_a.nrl.navy.mil
renate@meeker.ucar.edu	49	coetzee@aqua.ccwr.ac.za
hervig@dingo.uwyo.edu	14	coetzee@cirrus.sawb.gov.za
TOTALS:	60 users,	3976 accesses

FUNCTION	ACCESSES
plot_met	1622
<i>trajectory</i>	1357
metmaps	478
metprofile	329
<i>trajectory curt mail</i>	68
metxsects	67
curtain	33
nmc_status	22
TOTAL:	3976

This averages to about 11 jobs submitted per day. Emphasis denotes support by this IDS.

[Return to EOS page](#)